Effect of an isolated three-dimensional roughness element on the boundary layer transition to turbulence

Igor Braga de Paula, igorbra@gmail.com
USP - Escola de Engenharia de São Carlos - Depto. Engenharia de Materiais, Aeronáutica e Automobilística, Laboratório de Aerodinâmica. Av. Trabalhador Sancarlense 400, São Carlos, Brasil

Werner Würz, wuerz@iag.uni-stuttgart.de
Universität Stuttgart - Institute für Aerodynamik und Gasdynamik. Pfaffenwaldring 21, Stuttgart, Germany.

Márcio Teixeira de Mendonça, marcio_tm@yahoo.com
Centro Técnico Aeroespacial - Instituto de Aeronáutica e Espaço. Praça Mal. Eduardo Gomes, 50 - CTA/IAE/ASA-P, São José dos Campos, Brasil.

Marcello Augusto Faraco de Medeiros, marcello@sc.usp.br
USP - Escola de Engenharia de São Carlos - Depto. Engenharia de Materiais, Aeronáutica e Automobilística, Laboratório de Aerodinâmica. Av. Trabalhador Sancarlense 400, São Carlos, Brasil

Abstract. *The influence of a single 3-D roughness element on the evolution of a 2-D Tollmien-Schlichting (T-S) wave was studied in the current work. The effect of this type of disturbance on the flow stability is important for drag estimation of aircrafts, because the viscous and the pressure drag are influenced by the boundary layer transition. The experiments of the current work were carried out in a laminar wind tunnel with a turbulence level of 0.02% of the freestream velocity. This was an important feature because the noise level required for this kind of experiments is extremely low. In the current experiments the T-S waves were excited artificially with micro loudspeakers. The cylindrical roughness element used in the experiments was slowly oscillated as a quasi-steady disturbance. The oscillation of the roughness was synchronized with the T-S waves, therefore the signal from the hot-wire anemometry measurements could be ensemble averaged in order to improve the signal to noise ratio. The experimental results were compared with a theory proposed in the present work. The theoretical results were provided by a simulation using a numerical code based on the Parabolized Stability Equations (PSE) (Mendonça, 1997). The comparison of the proposed model and the experimental results showed a good agreement up to moderate roughness heights. It was concluded that the main influence of this type of disturbance results in the generation of oblique modes at the same frequency of the excited T-S wave. It was also found that the critical roughness height which can affect the boundary layer transition is dependent on the threshold for self-sustained fundamental resonance in the boundary layer.*

Keywords: *single roughness, Blasius, secondary instability, K-type*

1. INTRODUCTION

The current work consists in a study on the boundary layer transition induced by a single 3-D roughness element. Roughness elements are often found on aircrafts surfaces. It is well known that large part of the parasite drag of an aircraft is related to the boundary layer transition. According to Kundu et al. (2000), during the cruising regime of an aircraft the parasite drag corresponds to about 12% of the total drag. The drag is one of the main parameters related to aircrafts performace. As a consequence, the problem of early transition caused by roughness elements is being studied since the 1940's Tani and Hama (1940). Since then, the improvement in theory, numerical simulations and experiments led to a better understanding of the problem of the transition induced by roughness elements.

Actually, due to the advances on the study of such a problem, the scenario of early transition induced by roughness can be divided in three different classes namely small, medium and high roughness. These classes are related with the complexity of the phenomena that increases with the elevation of the roughness height. For roughness elements with very small heights, normally below 5% of the boundary layer displacement thickness (δ^*), the generation of instability waves, also known as Tollmien-Schlichting waves (Schlichting (1979)), is the main influence of the roughness on the boundary layer. In this regime, the roughness elements acts as a linear transformator of outher disturbances, such as sound and vorticity, into boundary layer instability waves. These waves have a wavelength completely different from their former disturbances. In the case where T-S waves are already present in the flow, these kind of roughness can induce a scattering of these waves into oblique ones Ustinov (1995). The evolution of the waves generated by both process then propagate as predicted by primary or secondary instability theory. The occurrence of the latter is conditioned to the sufficient high amplitude of the waves.

After the introduction of the receptivity concept by Morkovin (1968), many works were devoted to the study of the generation of instability waves by very shallow roughness elements. The development of the secondary instability theory

by Herbert (1988) helped to increase the amount of work related to the pure receptivity induced by roughness such as Choudhari and Kerschen (1990), Tadjfar and Bodonyi (1992) and Würz et al. (2003). This is due to the fact that the secondary instability theory could predict well the non-linear evolution of 2-D or 3-D T-S modes but not their origin. The estimation of the initial conditions of the waves would come from the receptivity. The scattering of the T-S waves due to very small roughness attracted almost no attention and Ustinov (1995) performed the unique study found in this regime.

As the roughness height increases and it enters in the class of medium roughnesses, its influence on the boundary layer transition adds some other effects. These effects are derived from the mean flow distortion caused by the roughness. The mean flow distortion can change considerably the quantity of energy that is converted into Tollmien-Schlichting waves. This can turn the receptivity process non-linear with respect to the roughness height variation. The mean flow distortion can also change the stability characteristics of the boundary layer downstream of the roughness. For two-dimensional roughness elements, the distortion of the boundary layer mean flow profiles and its consequent modification of the stability characteristics of the boundary layer, was the main effect that caused the anticipation of the transition Klebanoff and Tidstrom (1972). For three-dimensional roughness the structure of the mean flow formed in the wake of such elements was studied for example by Tani (1961), Sedney (1973), Tobak and Peake (1982), Gaster et al. (1994), Legendre and Werlé (2001). Those works provided a clear view of the vortex pattern in the roughness wake. The stability of these vortices was studied by Cossu and Brandt (2004), Jacobs and Durbin (2001). According to Cossu and Brandt (2004), the boundary layer in the wake of the roughness become inviscidly unstable when the mean flow distortion reach levels close to 26% of U_∞. In the case where the T-S waves are already existent in the flow, the three-dimensional mean flow distortion can induce additionally a deformation of the incoming waves into oblique waves. The occurrence of this effect was speculated in the works of Wang (2004) and Rist and Jäger (2004). However, no conclusive evidence was found in those works.

In a real situation even small disturbances are always present in the flow. Thus, all afore mentioned effects tend to occur together. In the previous performed works these effects have been investigated separately. Therefore, the most influent effects and the interaction of two or more effects could not be analyzed in detail. The aim of the current work is to shed some light on the transition mechanism that can be induced by a medium sized roughness element in a scenario where T-S waves are previously present in the flow. This can be a step toward the understanding of the third class of roughness that involves very high elements ($h \geq \delta^*$). The transition process in this case is very complex and often led to a the bypass. The works of Klebanoff et al. (1992) and Ergin and White (2006) have attempted to explain the mechanism of transition associated to such high roughness elements, but no conclusive result was found and the lack of theory to explain the transition mechanism induced by such roughness still remains.

2. METHODOLOGY

In the current work the effect of a medium sized roughness element on the evolution of instability waves already existent in the flow was studied. The main idea of the current approach is to use the boundary layer instability theories to analyze the evolution of the instability waves downstream the roughness. The hypothesis that is being checked in the present study is that a medium sized roughness would act as a seed of three-dimensionality in the boundary layer. Further on, this three-dimensionality can feed a secondary instability of the boundary layer. In this approach, if the amplitude is sufficient high to trigger the secondary instability, the outcome from the interaction of the roughness with a Tollmien-Schliching wave will be a resonance of K-type.

In order to check the proposed idea, an experiment was performed with a roughness element interacting with a controlled Tollmien-Schlichting wave, and the results were compared with the secondary instability theory. The results of secondary instability theory for a smooth flat plate were provided by the numerical solution of the parabolized stability equations (PSE). The numerical code used in the current work was developed by Mendonca (1997).

3. EXPERIMENTAL SET-UP

The experiments were carried out in the Laminar Wind Tunnel (LWT) Wortmann and Althaus (1964) at the University of Stuttgart. This wind tunnel is an open return tunnel. The rectangular test section has a cross section area of 0.73 X 2.73m^2. In this tunnel, for a speed of 30ms^{-1}, the free stream turbulence in the range of 20-5000Hz is lower than $0.02\%U_\infty$.

The experiments were performed on an airfoil model with a 600mm chordlength. The XIS40MOD section adopted was identical to that used in the controlled receptivity experiments, by Würz et al. (2003). This airfoil was chosen because, by just adjusting the angle of attack, it could provide a relatively long stretch of zero pressure gradient boundary layer in a region of negligible surface curvature. This enables the comparison of the results with theories or numerical simulations based on a Blasius boundary layer. A scheme of the experimental set-up used is shown in figure 1.

The controlled disturbances that produced the T-S waves were introduced into the flow by a slit source mounted flush to the airfoil surface. A similar arrangement was previously used in Würz et al. (2004). The disturbances to generate T-S waves were provided by 32 loudspeakers connected to a slit by equally spaced tubes. A total of 116 tubes were used to

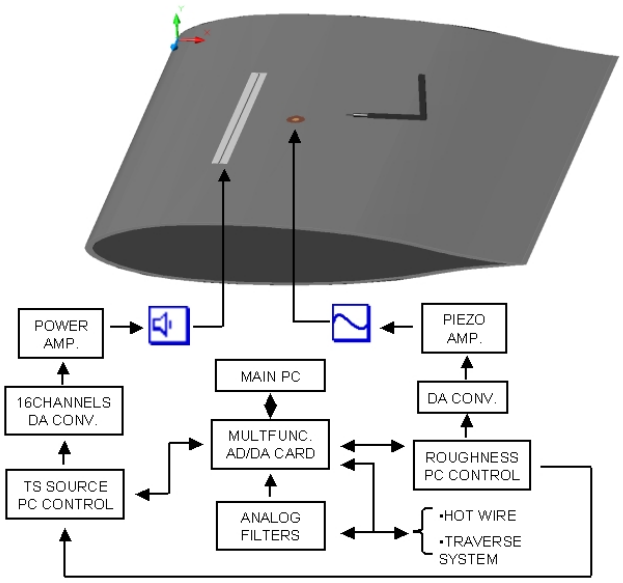

Figure 1. Experimental set-up

cover a spanwise range of 300mm of the airfoil surface.

The retractable roughness was mounted downstream of the T-S source. The position of this element and of the T-S slit source were chosen based in a careful analysis of many parameters. The parameters considered in this analysis were the extension of zero pressure gradient region on the airfoil, the Re_{δ^*}, the non-dimensional unstable frequencies within this region, the power of the T-S generator and the minimum distance to ensure a well developed T-S wave at the roughness. Several configurations were evaluated in order to optimize the experiment. Finally, the positions were fixed at 40% of the chord length for the roughness and 25% for the T-S generator. This corresponded to a distance of approximatelly nine T-S wave lengths, between the slit source and the roughness (region I in figure 2), and eleven wave lengths of zero pressure gradient downstream of the roughness (region II in figure 2).

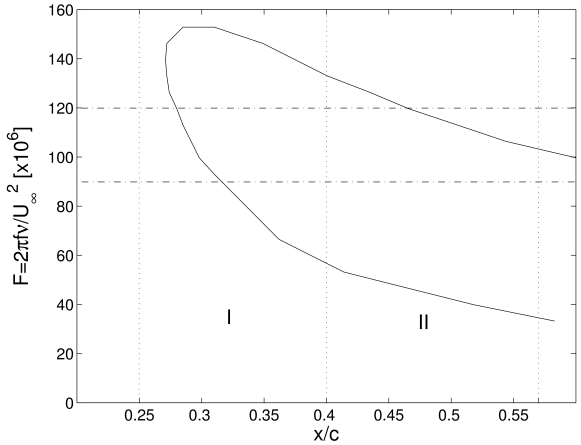

Figure 2. Stability diagram for two-dimensional TS-waves for the airfoil section used. I indicates the region between the slit source and the roughness, and II corresponds to the region of zero pressure gradient downstream the roughness. The Reynolds number based on the chord length used for the calculations was equal to $9,4 \times 10^5$.

The roughness element used was of a cylindrical shape with 10mm in diameter. It was placed at the spanwise center of the airfoil section at streamwise position equal to 40% of the chordlength. Prior to the experiment, the height of the roughness element was measured in place by a Micro-Epsilon optoNCDT 1605-0,5 which is an optoelectronic micrometer device. This micrometer has a static resolution of $0.1\mu m$ and can be used with frequencies up to 10kHz. The roughness height was driven by a piezo actuator, controled by an analog voltage input which was calibrated by the roughness height measurements. The Reynolds number ($Re_h = U(h)h/\nu$) related to the maximum roughness height used in the current work was approximately 60. This Reynolds number was calculated according to Ergin and White (2006). During the

experiments the roughness height was slowly oscillated with a frequency approximately 1500 times lower than the TS wave frequency. Therefore, it could be considered as a quasi-steady roughness.

The influence of the roughness height on the T-S waves evolution could be better analyzed by using the quasi-steady but oscillating roughness. This enabled the acquisition of data for many roughness heights in a relatively short time. In other words, this optimized the use of the tunnel time. It is also important to note the tunnel was of the open circuit type. In such type of tunnel is hard to control the environmental conditions during the experimental campaigns. However, for short time campaigns of approximately 8 hours, the experimental conditions can be well corrected imposing no significant influence on the results.

In the experiments of the current work all equipments were connected to each other via a controller computer. This was necessary for the synchronization of the experiment. This enabled, the acquisition to be triggered always at the same phase of both T-S wave and the roughness element. The configuration adopted also enabled the adjustment of the roughness initial position. Therefore, it was possible to optimize the time interval of the cycle during which the data was acquired. This was important because of the time necessary for the T-S wave to reach the hot wire probe. Thus, the first collected data points were discarded to avoid the influence of this start up transient.

The distance of the hot-wire from the wall was measured by slowly moving the probe until it touched the wall. By comparison with the Blasius velocity profile it was found that at this point the hot-wire was at 0,05mm from the wall. This offset was taken into account for the correct Y position evaluation. This procedure was carried out for every streamwise station. In the spanwise measurements the wall normal position was obtained based on measurements of the velocity profile. Assuming a Blasius boundary layer, for the cases with nominally zero roughness heights, the probe Y position could be adjusted very accurately and kept constant during the spanwise traverses.

4. OPTIMIZATION OF THE EXPERIMENTAL CAMPAIGNS

According to the results of Herbert (1988), the bandwidth of unstable 3-D modes ($\beta \neq 0$) due to secondary instability is dependent of the initial amplitude of the 2-D T-S waves involved in the process. Based on this result it was possible to devise a test to check the hypothesis proposed in the current work. This optimized the experiment and was extremely important because the time available for the test campaigns of the present work was very short.

The initial amplitude and frequency of the Tollmien-Schlichting waves were chosen from amplification maps of 3-D waves under secondary instability (figures 3 and 4). These maps show iso-contours of growth (n-factor) of oblique waves with respect to the initial amplitude of the 2-D T-S waves. The results shown in these figures were obtained by numerical simulations of the boundary layer secondary instability. A PSE code was used for these calculations. The non-dimensional frequencies used in the PSE runs of figures 3 and 4 were respectively $F = 2\pi f\nu/U_0^2 = 120 \times 10^{-6}$ and $F = 90 \times 10{-}6$. The numerical simulations were performed with conditions close to that of the experiments. The initial $Re_{\delta*}$ number used in the simulation was equals to 950, in the experiments this corresponds to a streamwise position close to the roughness. The Reynolds number at the end of the simulation was equals to 1180 which corresponds approximately to the last measurement station of the experiments.

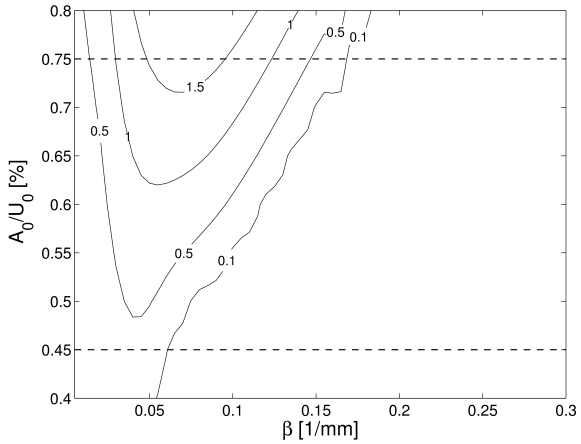

Figure 3. Amplification map of 3-D modes due to secondary instability. PSE calculations. F=120×10^{-6}.

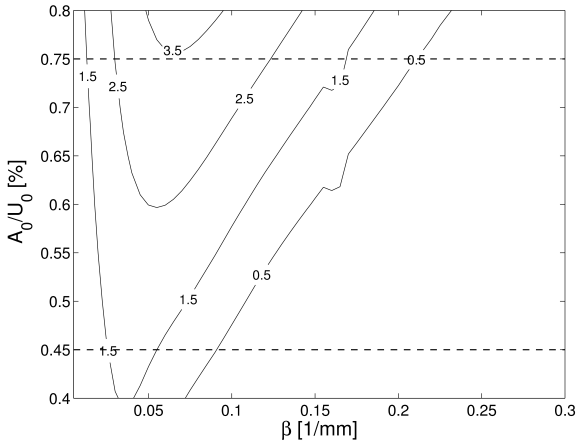

Figure 4. Amplification map of 3-D modes due to secondary instability. PSE calculations. F=90×10^{-6}.

The amplifications maps of figures 3 and 4 show significative differences on the growth of 3-D modes when the initial amplitude of the 2-D waves are either equal to 0,45% or to 0,75% of U_0. These amplitudes are marked in the figure by dashed lines. In figure 3, the theoretical map predicts a significant growth of 3-D modes for A_0 equals 0,75%U_0. On the other hand, for A_0=0,45%U_0 no significant growth of 3-D modes is predicted. In figure 4, the secondary instability theory predicts an amplification of oblique modes for both initial amplitudes. However, for A_0 equals 0,45%U_0 the bandwith of

unstable 3-D modes is located at smaller spanwise wavenumbers. Thus, if the hypothesis proposed in the current work is correct, the experiments at these four conditions would show different behaviours. This was considered enough to check the validity of the proposed physical model for the transition induced by medium sized roughness heights. The four cases covered in the experiment are listed in table 1.

Table 1. Cases covered in the current experiments.

CASE	FREQUENCY	A_0
1	$F = 120 \times 10^{-6}$	0,75%U_0
2	$F = 120 \times 10^{-6}$	0,45%U_0
3	$F = 90 \times 10^{-6}$	0,75%U_0
4	$F = 90 \times 10^{-6}$	0,45%U_0

5. CHARACTERISTICS OF BASE FLOW IN THE MEASUREMENT REGION

Prior to the main experiments, measurements were performed in order to adjust the airfoil angle of attack to obtain a sufficiently long stretch of zero pressure gradient boundary layer on the model surface. The velocity distribution was obtained from readings of 26 pressure taps. The hot wire traversing system was kept in place to take into account its influence on the circulation of the airfoil. From boundary layer measurements inside the studied region the Falkner-Scan parameter ($\Lambda = (dU/dx)\left(\theta^2/\nu\right)$) was calculated, as suggested in Schlichting (1979). The Falkner-Scan parameter is a measure of the effect of pressure gradient on the velocity profile. Where this parameter reaches values close to zero, it means that pressure gradient is negligible in this region. In the current experiments the Falkner-Scan values shown in figure 5 remained fairly small. This condition was obtained with an angle of attack of -3.2deg. The solid line shown in the figure corresponds to the velocity distribution predicted by simulations with the Xfoil.

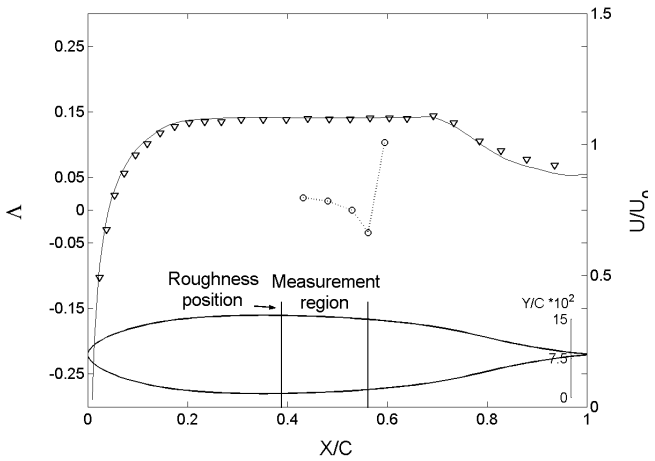

Figure 5. Velocity distribution - ∇ - and Λ - o -

The region where the measurements were carried out was also an important decision that had to be taken. By choosing a single distance from the wall (Y position) for the spanwise measurements it was possible to reduce considerably the time of the experimental campaigns. Thus, preliminary experiments were performed with the roughness in order to evaluate the possibility of choosing a single Y position for the spanwise traverses without any significant information losses.

The measured profiles of Tollmien-Schlichting waves downstream of the roughness for a medium roughness height are shown in figure 6. The experimental conditions used for these measurements were similar to those of the Case 1 (table 1). Figure 6 shows an increasing deformation of the profiles as the wave develops downstream of the roughness. Close to 0,75y/δ^* the distortion of the wave profile was more evident. This coincides with the peaks of the unstable oblique waves predicted by the secondary instability theory (map of figure 3). In view of these results, the non dimensional y position chosen for the spanwise traverses was 0,75δ^*. In the experiments performed with a non dimensional frequency of 90×10^{-6}, the height of the peaks of the unstable oblique modes was slightly different. In these cases the peaks where located close to 0,85δ^*. Thus, this non dimensional Y position was chosen for the spanwise traverses of Cases 3 and 4.

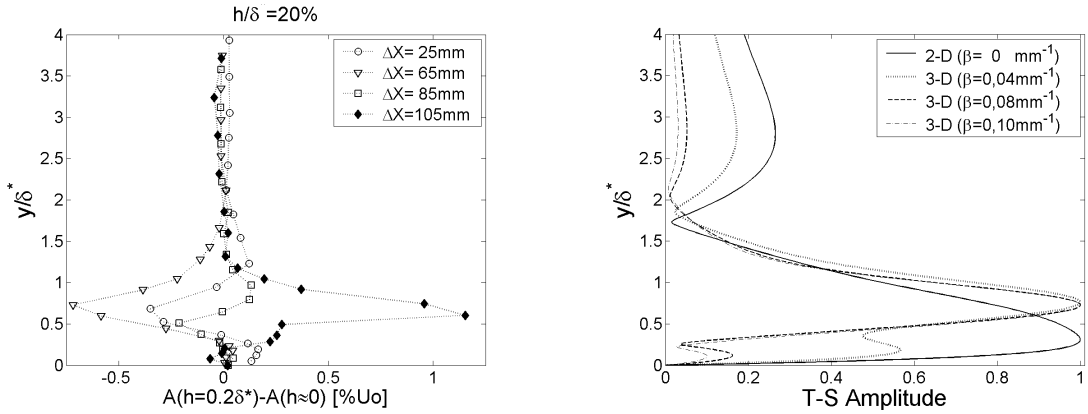

Figure 6. Left plot: Distortion of T-S wave amplitude profiles with respect to the case with nominally zero roughness height. Measurements carried out along the center line at different streamwise positions and with the experimental conditions of Case 1. Right plot: Eigenfunctions of a 2-D and some oblique T-S waves.

6. RESULTS

The measurements covered 70mm in the spanwise direction. These measurements were performed at several distances downstream of the roughness, namely 25, 45, 65, 85 and 105mm. The spacing between each spanwise position was approximately 1mm. The measurements of velocity fluctuation were interpolated through the measurement stations. Thus, a clear picture of the behavior of the T-S waves downstream the roughness was obtained.

Figure 7 show the evolution of the T-S waves for the Case 1 (see table 1). As the waves propagate downstream, it could be seen a growth of the 3-D structure which was formed by the interaction of the waves with the roughness. This behavior is consistent with the secondary instability predictions given by the map of figure 3. The amplitude of the 3-D structure have also increased with the roughness height. For small and medium roughness heights the evolution of the 3-D structure seemed to follow the same pattern. For high roughness the patterns was different and more complex. In this case at the last stations the flow may already be turbulent at the center line.

The evolution of the T-S waves downstream the roughness for the Case 2 is shown in figure 8. Within the experimental domain the growth of the 3-D structure downstream the roughness could not be seen. This occurred for all roughness heights shown in figure 8. Indeed, according to the amplification map of figure 3, for the Case 2, no significant growth of oblique modes would be expected due to secondary instability mechanism. Again, this is consistent with the experimental observations.

The evolution of the T-S waves measured downstream of the roughness for the Case 3 is shown in figure 9. In this case, as the waves propagate downstream a strong growth in the wave amplitude at specific regions along the spanwise direction occurs. For both small and medium roughness heights (approx. 20% of δ^* and below), the waves evolution seemed to follow a similar pattern. For large roughness heights the 3-D structure of the T-S waves that arose downstream the roughness have shown a different evolution. In this case the T-S waves evolved into a more complex structure. A similar behavior was observed for the Case 1.

According to the map of figure 4, for the Case 3 a strong amplification of oblique modes due to secondary instability mechanisms would be expected. The experimental data are consistent with expectation. The evolution of the T-S waves downstream the roughness at the conditions of Case 4 is shown in the plots of figure 10. The results suggests a small growth of the 3-D structure as the waves propagate downstream. The pattern of the T-S waves was roughly the same for all roughness heights shown in this figure. However, the structure of the T-S waves downstream of the roughness was different from those observed when the initial amplitude of the 2-D wave was higher (Case 3). According to the map of figure 4, for the Case 4 the growth of oblique modes due to secondary instability would occur in a bandwidth of 3-D modes different from that of Case 3. Thus, the experimental results are in qualitative agreement with the predictions.

For all cases analyzed the comparison of the experimental data with the secondary instability predictions showed a qualitative agreement. This supports the proposed model for the transition induced by roughness for the scenario of the present study. However, a more quantitative analysis can be performed to ensure the validity of the model. This quantitative analysis was done by comparison of the experimental and theoretical growth of the 3-D modes.

7. COMPARISON WITH THE PROPOSED MODEL

The growth and decay of 3-D modes was analyzed with aid of the spectrum of spanwise wavenumbers. The theoretical spectrum of spanwise wavenumbers was obtained by applying the experimental conditions to the PSE calculations. The

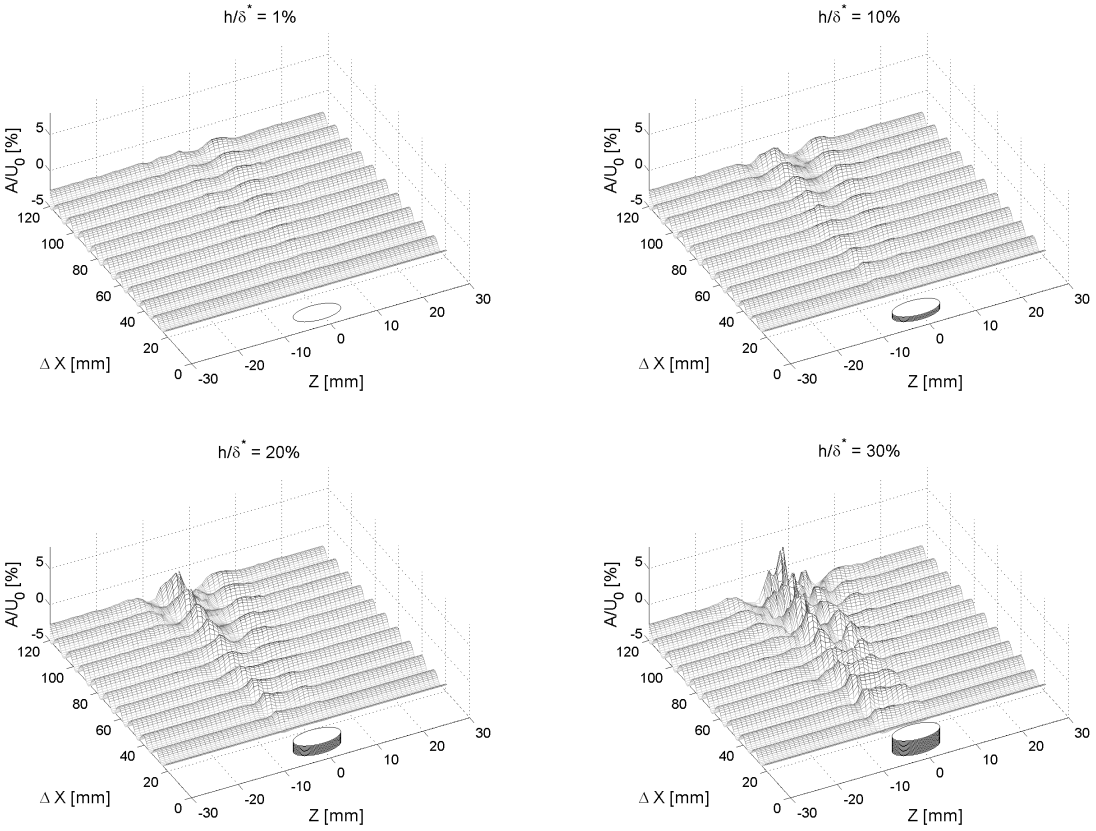

Figure 7. T-S waves evolution downstream of the roughness. Conditions of the experiment: Case 1.

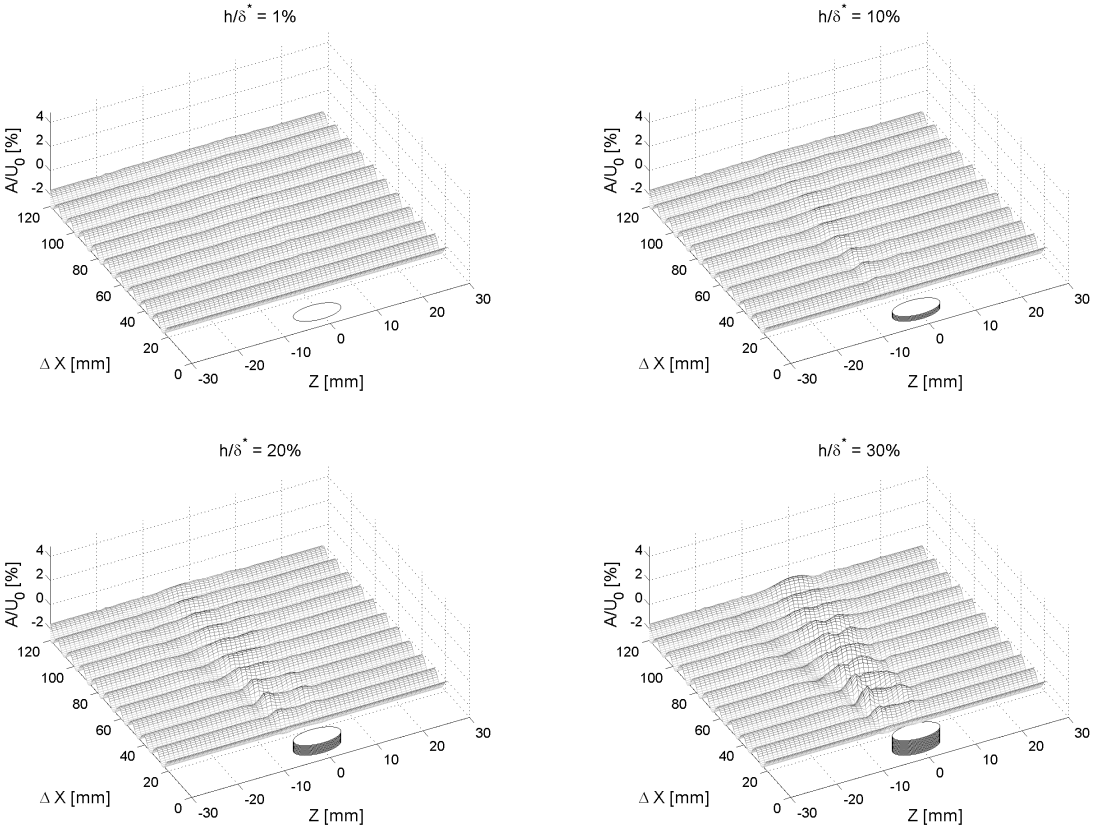

Figure 8. T-S waves evolution downstream of the roughness. Conditions of the experiment: Case 2.

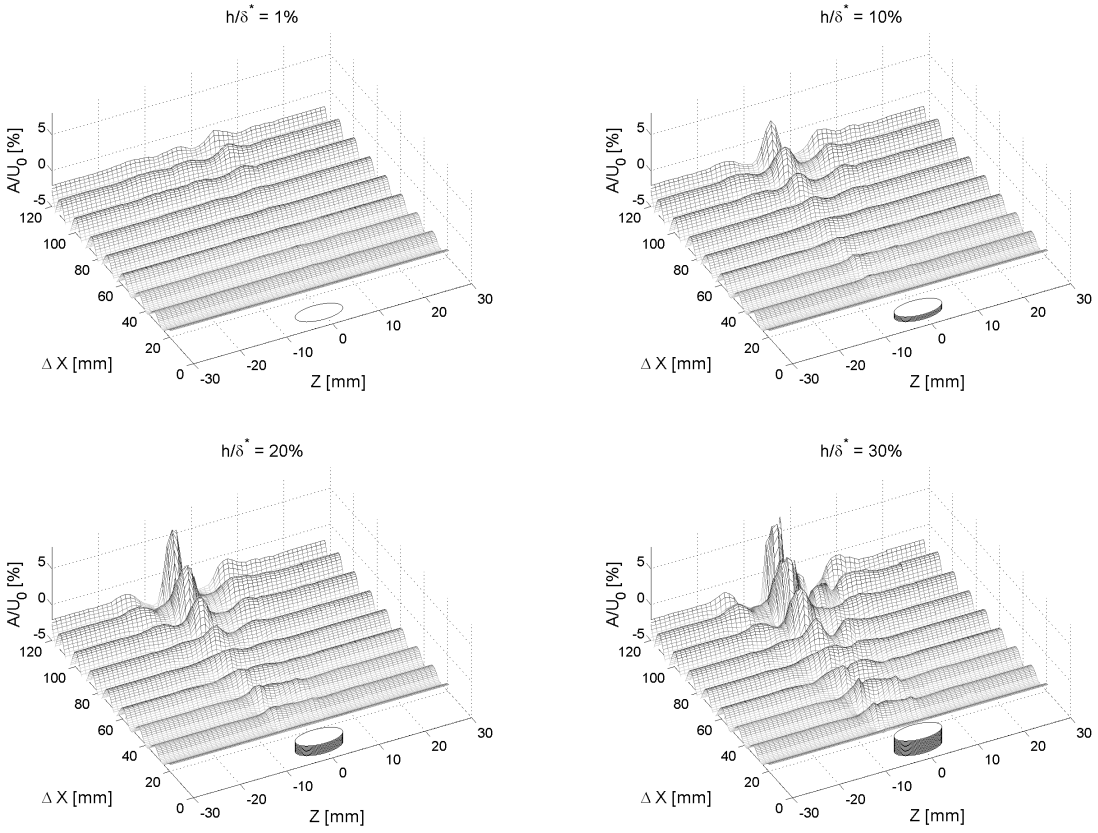

Figure 9. T-S waves evolution downstream of the roughness. Conditions of the experiment: Case 3.

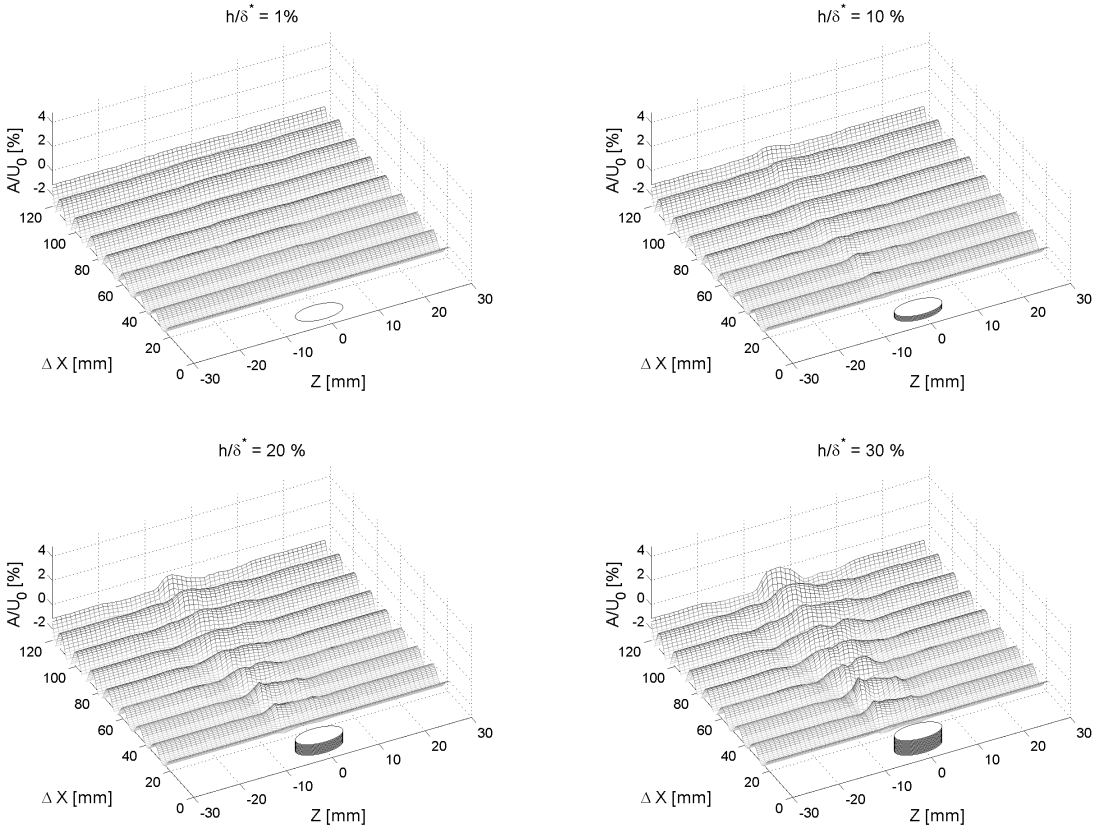

Figure 10. T-S waves evolution downstream of the roughness. Conditions of the experiment: Case 4.

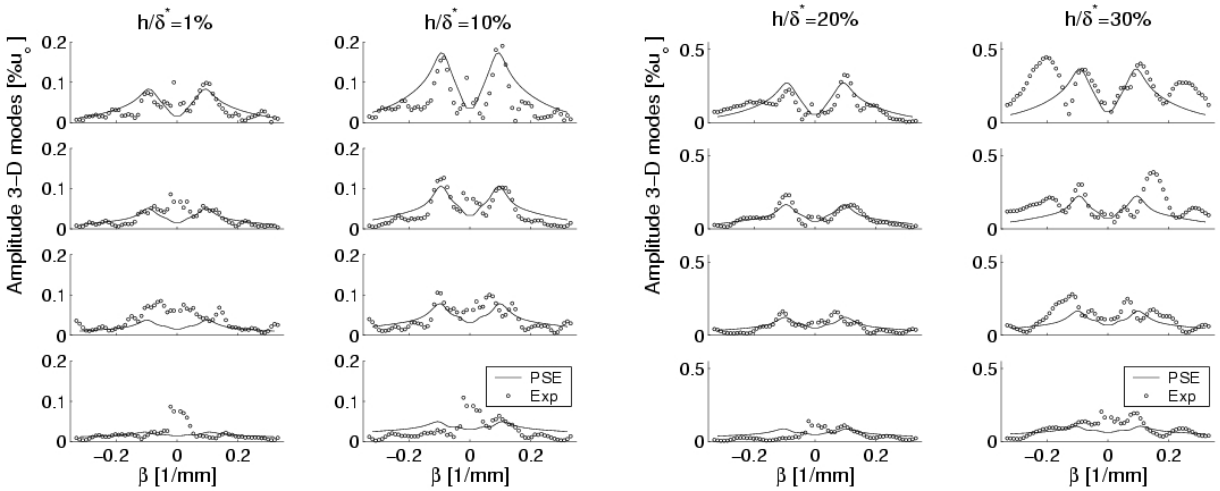

Figure 11. Comparison of the evolution of the spanwise wavenumbers spectrum. Solid line - predictions of the proposed model; Symbols - experiments. ΔX from bottom to top = 45, 65, 85 and 105mm. Conditions of the experiments: Case 1.

initial Reynolds number ($Re_{\delta*}$) used in the calculations was set to 870. In the experiments, this Reynolds number corresponds to a position located upstream the roughness. A position upstream the roughness was chosen in order to ensure a well developed calculation in the marching procedure used for solve the PSE equations. The Reynolds number step ($\Delta Re_{\delta*}$) adopted in this marching procedure was equals to 10. The Reynolds number at the end of the simulation was set to 1150. This Reynolds number corresponds to the last measurement station downstream the roughness.

For the comparison of the numerical calculations with the experiments it was first necessary to model the disturbances generated by the roughness. This was done by assuming that the disturbances generated by the roughness are restricted to a narrow spanwise region. A flat spectrum is a reasonable model for a signal that is confined in a very narrow window of the reference variable such as time or space. Therefore, it was assumed a flat spectrum for the numerical calculations of the secondary instability. The relevance of this simplification becomes lower as the growth due to the secondary instability increases. The flat spectrum was not set at the initial Reynolds number of the simulations. The spectrum was assumed as flat only at $Re_{\delta*}$ equals to 1000. This Reynolds number corresponds to a station located between 25 and 45 mm downstream the roughness. In the work de Paula (2007) it is shown that influence of the roughness near field was strong upstream this Reynolds number. Thus, only downstream this near field the results from secondary instability calculations could be compared with the experiments.

For the conditions of Case 1, the comparison of the experimental results with the proposed model showed a good agreement at the measurement stations more distant from the roughness(figure 11). The experimental data showed an asymptotic behavior toward the model predictions. In the stations closer to the roughness the agreement was poor and as the distance from the roughness was increased the agreement became better. This is because the growth of the 3-D modes with respect to the initial amplitudes was small at the stations close to the roughness. At these station the secondary instability mechanism was responsible for a small amplification of the 3-D modes. Further downstream from the roughness, the growth with respect to the initial amplitudes was very strong and then the amplification of the waves due to secondary instability became more evident. At the last measurement stations, the agreement of the experimental data with the predictions show clearly that secondary instability was the main cause of the growth of disturbances.

For high roughness heights the experimental spectrum of figure 11 presented a double peak structure. This behavior was not predicted by the model. In this case strong non-linear effects can take place. Therefore the weakly non-linear model would be not enough to predict these effects.

The growth of a similar three-dimensional structure of the T-S waves was also seen at the conditions of Case 3. Again, the spanwise spectrum of the T-S waves showed good agreement with the predictions of the proposed model (figure 12). As for Case 1, this agreement was more evident at stations distant from the roughness. This occurred for the same reason of Case 1.

For high roughness heights the spectrum of figure 12 showed a double peak structure at the least measurement station. This behavior was also seen with the conditions of Case 1. In both cases the non-linear effects were stronger when the roughness was high.

For Case 4 a good agreement was also seen between the model and the experimental results (figure 13). An important characteristic is the fact that the most unstable 3-D modes are concentrated in a bandwidth different from Cases 1 and 3. This behavior was well predicted by the proposed model. This is a strong evidence of the validity of the model. For the Case 4 a good agreement between the model and the experiments was also seen for high roughness heights. This suggests

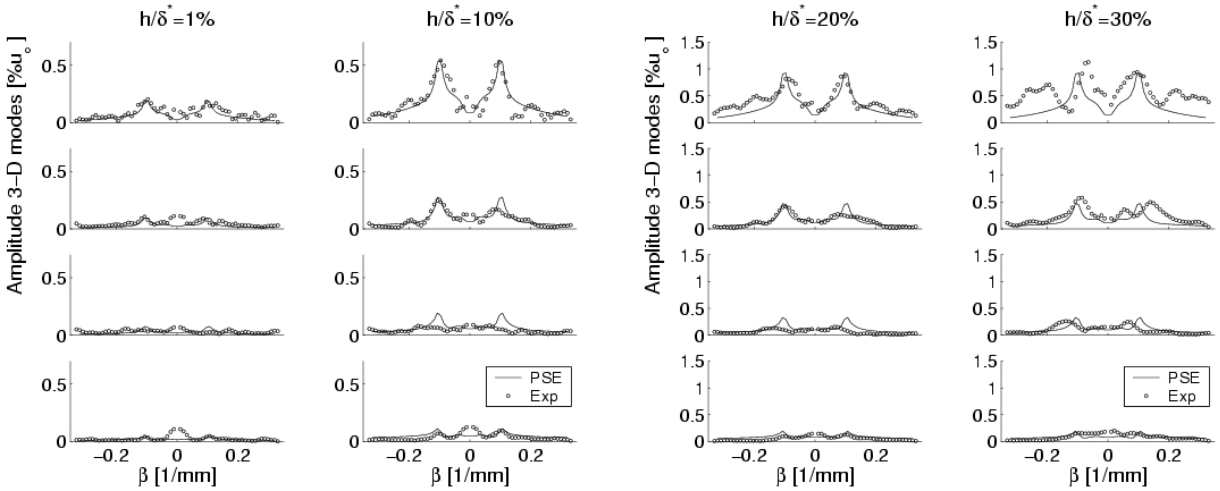

Figure 12. Comparison of the evolution of the spanwise wavenumbers spectrum. Solid line - predictions of the proposed model; Symbols - experiments. ΔX from bottom to top = 45, 65, 85 and 105mm. Conditions of the experiments: Case 3.

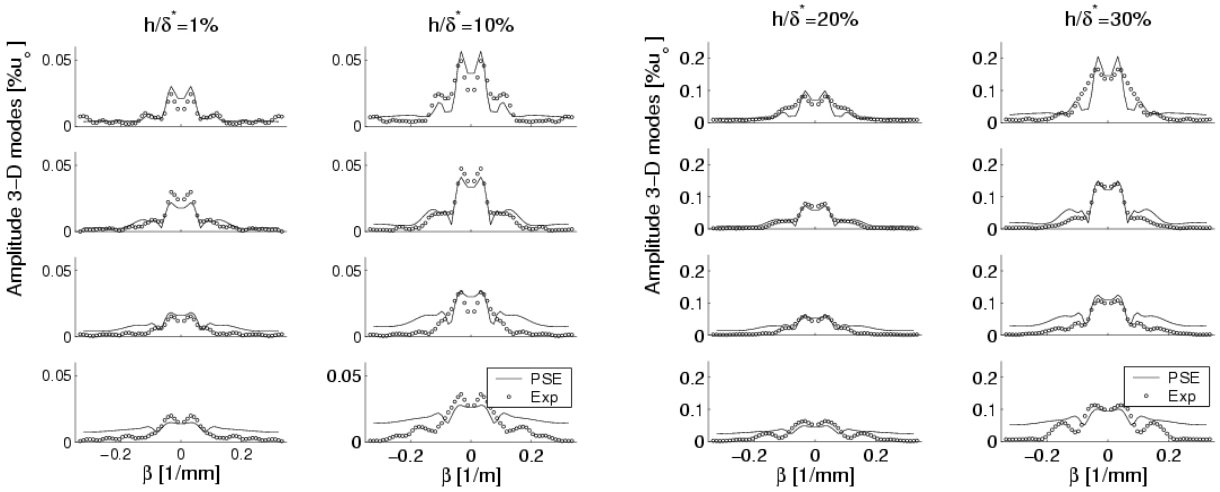

Figure 13. Comparison of the evolution of the spanwise wavenumbers spectrum. Solid line - predictions of the proposed model; Symbols - experiments. ΔX from bottom to top = 45, 65, 85 and 105mm. Conditions of the experiments: Case 4.

that the model can be valid even for high roughness heights, despite the bad agreement observed for high initial T-S wave amplitude. In the cases with high initial amplitude of the waves the fundamental resonance can still be responsible for the boundary layer transition. However, in these cases the weakly non-linear approach was not sufficient to model the physical problem.

8. CONCLUSIONS

The results presented concern a study of the effect that a 3-D shallow roughness element has on the evolution of 2-D T-S waves. In this paper some roughness heights were chosen and the results related to these cases were reported in some detail. In the current work a model was also developed that could predict a number of features of the transition induced by 3-D roughness elements. For the studied scenario, the proposed model is that roughness with small and medium heights are responsible for the seeds of three-dimensionality required to compose the triad resonant of the boundary layer secondary instability. In the present work, the calculations of the secondary instability were performed with a numerical solver of the Parabolized Stability Equations (PSE).

The results showed that the 3-D structure of the T-S waves downstream of the roughness was dependent on the initial amplitude of the 2-D T-S wave. The work showed that 3-D structure that develops downstream the roughness, followed a map of amplification of oblique modes, given by calculations of the secondary instability. Further on, more quantitative comparisons of the experimental results with the model predictions were performed. The results confirmed the validity of the proposed model for the studied scenario.

A practical result that can be extracted from the current work is related to the concept of critical roughness height, that can affect the location of boundary layer transition. The results of the current work show that the amplitude of the T-S waves are extremely important to evaluate the minimum roughness height that can affect the boundary layer transition. In the usual concept of critical roughness height, given initially by Tani (1961), just the boundary layer displacement thickness at the roughness location was considered.

9. ACKNOWLEDGEMENTS

This work was financially supported by FAPESP and CAPES.

10. REFERENCES

Choudhari, M. and Kerschen, E. J., 1990, Instability wave patterns generated by interaction of sound wave with three-dimensional wall suction or roughness, "AIAA", Vol. Paper No. 90-0119.

Cossu, C. and Brandt, L., 2004, On Tollmien-Schlichting-like waves in streaky boundary layers, "European Journal of Mechanics B/Fluids", Vol. **23**, pp. 815–833.

de Paula, I. B., 2007, "Influência de uma rugosidade tridimensional isolada na transição de uma camada limite sem gradiente de pressão", PhD thesis, Universidade de São Paulo, Escola de Engenharia de São Carlos, São Carlos, Brasil.

Ergin, F. G. and White, E. B., 2006, Unsteady and transitional flows behind roughness elements, "AIAA Journal", Vol. **44**, No. 11, pp. 2504–2514.

Gaster, M., Grosch, C. E., and Jackson, T. L., 1994, Velocity field created by a shallow bump in a boundary layer, "Physics of Fluids", Vol. **6**, No. 9, pp. 3079–3085.

Herbert, T., 1988, Secondary instability of boundary-layers, "Annual Review of Fluid Mechanics", Vol. **20**, pp. 487–526.

Jacobs, R. G. and Durbin, P. A., 2001, Simulations of bypass transition, "Journal of Fluid Mechanics", Vol. **428**, pp. 185–212.

Klebanoff, P. S., Cleveland, W. G., and Tidstrom, K. D., 1992, On the evolution of a turbulent boundary layer induced by a trhee-dimensional roughness element, "Journal of Fluid Mechanics", Vol. **237**, pp. 101–187.

Klebanoff, P. S. and Tidstrom, K. D., 1972, Mechanism by wich a two-dimensional roughness element induces boundary-layer transition, "Physics of Fluids", Vol. **15**, No. 17, pp. 1173–1188.

Kundu, A. K., Raghunathan, S., and Cooper, R. K., 2000, Effect of aircraft surface smoothness requeriments on cost, "The Aeronautical Journal", Vol. **104**, No. 1039, pp. 415–420.

Legendre, R. and Werlé, H., 2001, Toward elucidation of three–dimensional separation, "Annual Review of Fluid Mechanics", Vol. **33**, pp. 129–154.

Mendonca, M. T., 1997, "Numerical analisys of Görtler vortices Tollmien–Schlichting waves interaction with a spatial nonparalel model", PhD thesis, The PennState University, U.S.

Morkovin, M. V., 1968, Critical evaluation of transition flow laminar to turbulent shear layers with emphasis of hypersonically traveling bodies, "AFFDL TR", pp. 68–149.

Rist, U. and Jäger, A., 2004, Unsteady disturbance generation and amplification in the boundary-layer flow behind a medium sized roughness element, "IUTAM Symposium on laminar-turbulent transition".

Schlichting, H., 1979, "Boundary layer theory", McGraw Hill, 7^{th} edition.

Sedney, R., 1973, A survey of the effetcs of small protuberances on boundary-layer flows, "AIAA Journal", Vol. **11**, No. 6, pp. 782–792.

Tadjfar, M. and Bodonyi, R. J., 1992, Receptivity of a laminar boundary layer to the interaction of a three-dimensional roughness element with time-harmonic free-stream disturbances, "Journal of Fluid Mechanics", Vol. **242**, pp. 701–720.

Tani, I., 1961, Effect of two–dimensional and isolated roughness on laminar flow, "Boundary Layer and Flow Control–Pergamon Press", Vol. **2**, pp. 637–656.

Tani, I. and Hama, R., 1940, On the permissible roughness in the laminar boundary layer, “Rep. Aeronautical Research Inst. of Tokyo Imperial University”, Vol. **199**, pp. 419–429.

Tobak, M. and Peake, D. J., 1982, Topology of three-dimensional separated flows, “Annual Review of Fluid Mechanics”, Vol. **14**, pp. 61–85.

Ustinov, M. V., 1995, Secondary instability modes generated by Tollmien-Schlichting wave scattering from a bump, “Theoretical and Computaional Fluid Dynamics”, Vol. **7**, pp. 341–354.

Wang, Y. X., 2004, “Instability and transition of boundary layer flows disturbed by steps and bumps”, PhD thesis, Queen Mary College, University of London, U.K.

Wortmann, F. X. and Althaus, D., 1964, Der Laminarwindkanal des Instituts fĺur Aerodynamik und Gasdynamik der Technischen Hochschule Stuttgart, “Z. Flugwiss”, Vol. **12**, No. 4.

Würz, W., Herr, S., Wörner, A., Rist, U., Wagner, S., and Kachanov, Y. S., 2003, Three-dimensional acoustic-receptivity of a boundary layer on an airfoil: experiments and direct numerical simulations, “Journal of Fluid Mechanics”, Vol. **478**, pp. 135–163.

Würz, W., Sartorius, D., Wagner, S., Borodulin, V. I., and Kachanov, Y. S., 2004, Experimental study of weakly nonlinear interactions of instability waves in a non self-similar boundary layer on an airfoil - Part I: Base flow and initially tuned resonances, “12th International Conference on Methods of Aerophysical Research - ICMAR2004”, Novosibirsk.